DOE/METC/C-96/7224

Title:

Measurements of Coal Particle Shape, Mass and Temperature Histories: Impact of Particle Irregularity on Temperature Predictions and Measurements

Authors:

Ramanathan Sampath
Daniel J. Maloney
John W. Zondlo
Steven D. Woodruff
Yaw D. Yeboah

Conference Title:
26th International Symposium on Combustion

Conference Location:
Naples, Italy

Conference Dates:
7/28/96 to 8/2/96

Conference Sponsor:
The Combustion Institute

DISCLAIMER

This report was prepared as an account of work sponsored by an agency of the United States Government. Neither the United States Government nor any agency thereof, nor any of their employees, makes any warranty, express or implied, or assumes any legal liability or responsibility for the accuracy, completeness, or usefulness of any information, apparatus, product, or process disclosed, or represents that its use would not infringe privately owned rights. Reference herein to any specific commercial product, process, or service by trade name, trademark, manufacturer, or otherwise does not necessarily constitute or imply its endorsement, recommendation, or favoring by the United States Government or any agency thereof. The views and opinions of authors expressed herein do not necessarily state or reflect those of the United States Government or any agency thereof.

MASTER

DISTRIBUTION OF THIS DOCUMENT IS UNLIMITED

DISCLAIMER

This report was prepared as an account of work sponsored by an agency of the United States Government. Neither the United States Government nor any agency thereof, nor any of their employees, makes any warranty, express or implied, or assumes any legal liability or responsibility for the accuracy, completeness, or usefulness of any information, apparatus, product, or process disclosed, or represents that its use would not infringe privately owned rights. Reference herein to any specific commercial product, process, or service by trade name, trademark, manufacturer, or otherwise does not necessarily constitute or imply its endorsement, recommendation, or favoring by the United States Government or any agency thereof. The views and opinions of authors expressed herein do not necessarily state or reflect those of the United States Government or any agency thereof.

This report has been reproduced directly from the best available copy.

Available to DOE and DOE contractors from the Office of Scientific and Technical Information, 175 Oak Ridge Turnpike, Oak Ridge, TN 37831; prices available at (615) 576-8401.

Available to the public from the National Technical Information Service, U.S. Department of Commerce, 5285 Port Royal Road, Springfield, VA 22161; phone orders accepted at (703) 487-4650.

MEASUREMENTS OF COAL PARTICLE SHAPE, MASS AND TEMPERATURE HISTORIES: IMPACT OF PARTICLE IRREGULARITY ON TEMPERATURE PREDICTIONS AND MEASUREMENTS

by

Ramanathan Sampath[1,*], Daniel J. Maloney [2], John W. Zondlo[3], Steven D. Woodruff [2]
and Yaw D. Yeboah[1]

[1] Department of Engineering, Clark Atlanta University, Atlanta, GA 30314, USA
[2] U. S. Department of Energy, Morgantown Energy Technology Center, P. O. Box 880, Morgantown, WV 26507-0880, USA
[3] Department of Chemical Engineering, West Virginia University, Morgantown, WV 26505, USA

[*] Corresponding author, phone:(404)880-6733; fax:(404)880-6890; e-mail: rsampath@cau.edu

Submitted April 1996

The Twenty-Sixth International Symposium on Combustion
Naples, Italy
July 28 - August 2, 1996

Length of the Paper: 5496 words
Abstract: 217 words

	Words
Text (including references)	4058
Equations 5 x 21	105
Nomenclature Lines 19 x 7	133
Table 1 x 200	200
Figures 5 x 200	1000
Total	5496

Colloquium Topic Area: Coal and Organic Substances

ABSTRACT

Individual coal and carbon particles were levitated in an electrodynamic balance (EDB) and characterized using high-speed diode array and video based imaging systems to determine particle surface area, volume, drag, mass and density. These same particles were then heated bidirectionally using a long pulsed Nd:YAG laser to simulate combustion level heating fluxes (heating rates on order of 10^4 to 10^5 K/s). Measurements of particle surface temperature, size and laser temporal power variation were made and recorded during each heating experiment. Measured temperature histories were compared with a heat transfer analysis that accounted for variations in particle shape, mass, density, and laser heating power. Results of this study indicate that with well characterized materials of known properties agreement between measurement and model of within 20 K is typical throughout an entire heating and cooling profile. Large particle to particle variations are observed in coal particle temperature histories during rapid heating. These variations can be explained in large part by accounting for particle to particle property (shape, mass and density) variations. Even when accounting for particle to particle shape and density variation, however, model predictions greatly underestimate observed temperature histories. It is concluded that these discrepancies are largely due to uncertainties in the thermal properties (heat capacity and thermal conductivity) typically used to model coal combustion behavior.

INTRODUCTION

Recently Maloney et al. [1], reported results of an investigation to determine temperature histories for coal particles during the early stages of heating and devolatilization. In addition to making in-situ temperature measurements, they modeled the early stages of the heating process using thermal property correlations and spherical shape assumptions that are routinely applied to coals. Their predicted temperature transients agreed well with measurements for carbon spheres during the early stages of heating. However, for coal particles their predicted temperature transients differed significantly from measurements, with the measured temperatures being higher (by a factor of 2). Significant underprediction of heating rates for coal particles have also been noted in the work of Solomon et al. [2] and Fletcher [3]. The experiments of Maloney et al. [1] were conducted in a radiative heating/convective cooling environment, whereas the studies of Fletcher [3] were conducted in a convective heating/radiative cooling environment. This fact coupled with additional analysis led Maloney et al. [1] to conclude that the difference between measured and predicted temperatures were due to uncertainties in the relevant coal thermal properties and failure to account for particle shape factors.

During rapid heating, prior to devolatilization, the size and mass of coal particles remain unchanged for the first several milliseconds [1,4]. Therefore, the prediction of the temperature history prior to devolatilization requires knowledge of particle size, mass and thermal properties. Unfortunately, coal particles are irregular in shape and have unique external surface area, volume, mass and density [4-6]. While energy absorption and emission mechanisms depend on particle surface area (S), the temperature response depends strongly on particle mass (ρv). So, the shape and density of individual coal particles need to be addressed carefully in any heat transfer analysis. The assumption of spherical shape can result in underestimation of particle surface area because, for example, if the shape of the particle is assumed to be a parallelepiped, cylinder, cube, or ellipsoid of equal volume, then it has a surface area larger than that of a sphere of equal volume. Also, a spherical shape assumption with the size determined from one view of the particle or with a sieve mean size can overestimate the particle volume and hence the mass, which in turn would lead to underestimation of the predicted temperature histories. Hurt and Mitchell [7] reported large particle to particle temperature variations in their combustion studies of single char particles. They concluded that particle to particle variations in physical properties are a leading cause of these large temperature differences. Thus accounting for shape, mass, and density in the energy balance is a critical first step in modeling the temperature profiles of irregular particles. In the present work, recently developed methods were applied to measure the shape and mass of single irregularly shaped particles prior to heating.

Sampath [4] demonstrated shape and mass measurement capabilities for single irregular particles in an electrodynamic balance (EDB). Shape measurement involved viewing the particle at right angles using two video cameras and measuring breadth (B), thickness (T) and length (L) of the particle. Using this BTL information, the surface area and volume of the single particles were estimated. Following the approach of Maloney et al. [8], Sampath [4] also measured the drag coefficient/mass ratio (C_d/m) for coal particles in the EDB from the trajectory of the particle that resulted from an applied stimulus. Knowing the surface area and projected area of the particle perpendicular to the motion during the trajectory, the drag coefficient was determined independently based on Stokes Law. The mass of the particle was then separated from the C_d/m ratio. From the mass and volume, the density of the individual particles was obtained. The mean mass of a large number of single particles thus obtained using the EDB was then validated with the mean mass of several thousand coal particles obtained using an independent counting and weighing technique as described by Monazam and Maloney [6].

Maloney et al. [5] developed a more sophisticated 3D shape measurement technique by rotating the particles about the EDB center axis using a set of tangentially directed gas jets. As the particle rotated, a video-based imaging system recorded the particle images and stored perimeter data from successive video fields. Rotation rates were measured with the aid of a second video system positioned above the balance. Surface areas and volumes were calculated by summing the surface and volume elements swept out during rotation from one video field to the next. Surface area and volume data were then used to estimate the particle drag coefficient by applying an analysis for deformed spheres derived by Brenner [9]. The particle mass was calculated based on the measured C_d/m and the calculated drag coefficient [6].

In the present paper 3D shape, mass and density for a large number of coal particles were measured. The same particles were then radiatively heated and their temperatures measured during the subsequent heating and cooling. Particle temperatures were modeled incorporating measured particle shape and mass in the heat transfer analysis. Similar measurements were also made for carbon spheres to test the reproducibility of the temperature measurement system and to validate the numerical analysis presented in this work. The effect of shape and density on the temperature histories of coal particles is assessed by comparing model calculations using measured shape and density with that using a simple equivalent sphere method and uniform density assumptions.

EXPERIMENTAL METHODS

The present study is unique in that detailed measurements are performed on coal particle volume, external surface area, mass, density, laser incidental area, radiant energy flux, and transient temperatures during heating and cooling.

Measurement of Particle Volume, External Surface Area, Mass, and Density

Individual coal or carbon particles were levitated in an electrodynamic balance (EDB) and characterized using high-speed diode array and video based imaging systems. Fig. 1 shows the top view of the experimental system with the EDB represented by the small circle at the center of the figure. An individual particle is backlit with a red He:Ne laser at the side and with a light-emitting diode (LED) from the bottom of the balance. The magnified shadow image of the side view is split and projected onto the detector of a CCD video camera imaging system and a high-speed diode array imaging system (Fig. 1). The magnified shadow image of the bottom view is projected onto the detector of a second CCD video imaging system positioned above the balance.

The side view video imaging system was used to obtain the particle diameter for carbon spheres based on the projected image of the particle. The diode array imaging system was used to measure particle trajectory resulting from an applied stimulus. The drag coefficient/mass ratio (C_d/m) was obtained by matching the measured particle trajectory with the predictions from a simple force balance model [8] referred to as the Particle Dynamic Model (PDM). The PDM accounts for field forces, gravitational forces and drag forces acting on a charged particle during its motion in the EDB. For spherical particles, the equivalent diameter for predicting drag, projected area, surface area or volume diameter are the same. From the measured size and C_d/m ratio, the mass of individual carbon spheres was calculated. Finally, from the mass and volume, the density of the carbon sphere was determined. The reader is referred to reference [8] for complete details.

Following the approach of Maloney et al. [5], volumes and external surface areas were obtained for individual coal particles by rotating the particles and recording image data from successive video fields as a function of rotation angle. Measured surface area and volume were used to estimate particle drag coefficient as described by Monazam et al. [6], and the particle mass was then separated from the C_d/m ratio. From the mass and volume, the particle density was determined.

Measurement of Laser Incidental Area, Temperature and Laser Parameters

Single particles were heated bidirectionally. The actual cross-sectional area of the coal particle upon which the laser beam was incident (A_L) was also measured. This area was used to calculate the energy absorption response of the particle in the heat transfer analysis. The two opposite access ports for the heating beam were located at 60° counterclockwise and 120° clockwise to the access port for the side-view imaging system (see Fig. 1). A stable side-view cross-section of the particle prior to heating was measured and was used as a reference area. The laser incidental area (A_L) was determined from the particle cross-sectional area data which was measured as a function of rotation angle. This was done by locating the reference area in the rotational data and extracting the laser incidental area by going backward 60°. The same area was confirmed by going forward 120° from the reference area.

Following the measurements of particle shape, mass, reference area, and laser incidental area, the particle was heated from opposite sides with pulsed Nd:YAG laser beams of equal intensity. Experiments were performed in a nitrogen atmosphere. The temporal power variation in the laser pulse was recorded for use in the heat transfer analysis by an ultra-fast fiber optic ultraviolet light transmitter included in the beam path and coupled to a silicon photodiode (Fig. 1). Details of the laser power characterization are provided elsewhere [4,12]. Measurements of changes in particle size that accompany rapid heating were made by means of the high-speed diode array imaging system [1]. Measurements of the surface temperatures of the heated particles were performed using a single-wavelength pyrometer (see Fig. 1). Temperatures were determined based on measurements of particle size and radiant emission intensity with the application of Wein's approximation to Planck's law. The pyrometer was calibrated against a standard General Electric tungsten strip lamp to a temperature greater than 1500 K with an accuracy of ± 4 K. Signal-to-noise level for the pyrometer output exceeded 25:1 at temperatures above 800 K at the gain level employed in this work. Details of the pyrometer calibration are provided in reference [4]. Photographic records of the particle behavior during heating were also obtained. These records provided excellent time resolution of the particle response, including rotation, swelling, volatile evolution and the time at which the particle began to move off the imaging system array [1,4].

Measurements were made on individual particles of Spherocarb (Foxboro, Analabs, North Haven, CT), a spherical, nonfriable, microporous molecular sieve carbon sphere of mesh size 100/120 and PSOC-1451D a HVA bituminous coal in the aerodynamic size range of 106 - 125 μm. Spherocarb and PSOC-1451D coal were both used in previous studies by Fletcher [3] and Maloney et al. [1] and the same materials were used here so that the differences seen in both the present work and previous work could be examined.

ANALYSIS

One approach to predict temperatures for irregular particles of arbitrary shape is the equivalent volume sphere approximation. Here the temperature is calculated for a sphere with volume and mass (ρv) equal to that of the irregular particle. In addition, the energy absorption response is determined using the measured cross-sectional area, A_L, incident to the laser beam. The emission response is calculated using the measured particle surface area, S_p. Heat is assumed to flow only in the radial direction of the volume equivalent sphere. The model described here is influenced by the previous model developed by Maloney et al. [1], but it has been modified to include the particle volume, density, surface area, laser incidental area, and transient laser power (I(t)). As a base case condition, calculations were performed using the Merrick model to assign particle heat capacities [10]. Thermal conductivities were assigned using data for coals and chars of Badzioch et al. [11].

Particles were heated with laser beams of equal intensity from two sides. It is assumed that the particle absorbs a fraction of the energy proportional to its absorptivity ($\propto = 0.85$), distributes this energy uniformly throughout its entire surface and exchanges heat with the surrounding air. While heating, it is assumed that the particle retains its shape with no swelling, no rotation, and no mass loss. With the above restrictions, the temperature profile of the heating particle was obtained by solution of the Fourier equation for a sphere as,

$$\rho_p C_p(T) \frac{\partial T}{\partial t} = K_p(T) \left(\frac{\partial^2 T}{\partial r^2} + \frac{2}{r} \frac{\partial T}{\partial r} \right) \tag{1}$$

The following boundary conditions were applied:

(i) The initial condition at $t = 0$:

$$T(r,0) = T_o \qquad 0 \le r \le R \tag{2}$$

(ii) The symmetry condition at the center $r = 0$:

$$\frac{\partial T(0,t)}{\partial r} = 0 \qquad t \ge 0 \tag{3}$$

(iii) The energy delivered at the surface $r = R$:

$$K_p(T) \frac{\partial T(R,t)}{\partial r} = \left(\frac{2 A_L \alpha I(t)}{S_p} \right) - [h(t) \{T_s - T_\infty\} + \sigma \in \{T_s^4 - T_\infty^4\}] \tag{4}$$

The left hand-side of Equation 4 represents heat transfer to the particle interior by conduction from the surface while the first term on the right-hand side accounts for heat input by radiation, the second and third terms for cooling by convection and radiation respectively. The measured transient laser intensity, I(t), was used as the temporal laser input flux in the source term. This input flux was divided by a factor, $S_p/2A_L$, to account for the two-sided heating employed in the experimental system which gives a heating cross-section of $2A_L$. The convective and radiative cooling terms were considered using the measured external particle surface area.

The transient heat transfer coefficient, h(t), was determined from the transient Nusselt number, Nu(t), derived by solving the partial differential equation describing the unsteady temperature in the surrounding fluid and is given below [4]:

$$Nu(t)\big|_{r=R} = 2R\left(\frac{1}{R} + \frac{1}{[\pi k(T)t]^{\frac{1}{2}}}\right) \tag{5}$$

Here, k(T), is temperature-dependent thermal diffusivity of the surrounding gas (N_2) that was used to rotate the particle during the measurement of its shape. A numerical solution for Equations 1 to 5 was obtained [1] using an implicit Crank-Nicholson scheme since it is a nonlinear unsteady-state heat conduction problem involving the temperature to the fourth power in Equation 4.

RESULTS AND DISCUSSION

Validation with Carbon Spheres

The reproducibility of the temperature measurement and the validity of the numerical analysis were first tested using carbon spheres. Temperature traces of heating and cooling for replicate experiments on one carbon sphere are presented in Fig. 2. The data for this figure were obtained by heating the particle with a laser pulse, rebalancing the particle, repeating size, C_d/m and ρ measurements and then reheating the particle. For the data shown in Fig. 2, the same particle was rebalanced and reheated six times. The particle was heated with heating pulses of similar magnitude. The surface temperature of the particle and the transient power of the heating pulse were also measured. The data for the particle diameter, C_d/m, mass, and density showed little change from heating pulse to heating pulse and were respectively 135 μm, 21.5, 1.07 μgm, and 0.83 g/cm^3. It was seen that in all these experiments, the DC endcap voltage required to balance the particle remained almost the same. This suggests little change in particle mass for the carbon sphere during these experiments, since the DC endcap voltage is directly proportional to the particle mass. As illustrated, the measured temperature histories were all very similar. The heating rate employed in these experiments was ~8 x 10^4 K/s and the heating pulse time-averaged intensities (I(ta)) for these experiments varied only slightly from 600 to 650 W/cm^2. The dashed lines in Fig. 2 are the model predictions for the upper and lower bound (highest and lowest heat flux cases) for the experiments shown. Based on similar experiments, Maloney et al. [1] showed good agreement between measurement and model over the first 6 ms of heating for carbon spheres but then observed significant differences between model and measurement during the later stages of heating. The refinements made in the present work, in particular the inclusion of a time dependent heat flux in the energy balance, enable an excellent match between model and measurement over the entire heating and cooling profile for the carbon spheres. The seven temperature profile curves presented in Fig. 2 indicate a spread of from 20 to 50 K in temperatures at any given point in time for the six replicate experiments. The dashed lines in the figure illustrate model results for the two extreme (highest and lowest) heat flux experiments. These curves define a band of temperatures with a spread from 20 to 40 K between the two curves. This comparison illustrates that most of the variation seen in Fig. 2 can be accounted for by variations in heat flux. The energy balance applied in this work can match measured temperatures to within ± 20 K over the entire range of heating and cooling. These results validate the numerical analysis presented above for carbon spheres and indicate that for spheres with well known properties we have a good handle on modeling heat transfer.

Assessment of Coal Particle Shape and Density

Experiments were conducted on single bituminous coal particles for a range of heating rates (10^4 - 10^5 K/s) up to a surface temperature of about 1600 K. Four different time-averaged intensity levels (228-298, 553-707, 927-1104, and 1314-1380 W/cm^2) were employed to heat the particles. The shape information (equivalent diameters for particle surface area, volume, side projected area, and laser incidental area), the particle C_d/m, mass and density, and the time-averaged intensity of the various heating pulses are presented in Table 1. The mean surface area and volume equivalent diameters, C_d/m, mass, and density for 39 coal particles tested are in good agreement with the results obtained for 23 particles of the same coal by Monazam et al. [6]. The wide range of values seen in the surface area diameter, volume diameter, and density between coal particles suggest that when subjected to similar heating environments, the temperature response for these particles would vary significantly. This point will be illustrated more clearly in the discussion of figures 3 through 5 below.

In this section the effect of including measured particle shape and density on calculated temperature histories is assessed relative to the assumptions of spherical particle shape and uniform density taken from the literature. The model containing these spherical shape assumption is referred to as the 'base case' study. Predicted temperatures are calculated first for the base case and next using the actual measured coal particle shape and density. A comparison is made between these predictions and the measured temperatures. Following the work of Maloney et al. [1], the volume and surface area of the particle were calculated for the base case using the same cross-sectional area equivalent diameter measured from the side-view of the particle (provided in Table 1). The density of the coal particles was assumed to be 1.2 g/cm^3, a value taken from the literature [1,3]. Following this calculation, the actual measured surface area, volume, laser incidental area, and density were used to predict the temperatures for the second case. In both cases, Merrick's "Two Characteristic Temperature Equation" [10] was used to calculate the instantaneous heat capacity. The thermal conductivity was estimated using an equation fitted to the temperature-dependent data for coals of Badzioch et al. [11]. Also, constant mass was assumed throughout.

In Fig. 3, the base case prediction for one coal particle (number 16 of Table 1: d_v=93 μm, ρ=1.2 g/cm^3, $S_p/2A_L$=2, and I(ta)=941 W/cm^2) during its heating and cooling is compared with the prediction using the actual measured shape and density (d_v=98 μm, ρ=1.16 g/cm^3, and $S_p/2A_L$=1.9). The experimental temperatures are also shown in Fig. 3 for comparison. It should be noted that the pyrometer has a lower threshold limit about 800 K and temperatures less than 800 K are indications of pyrometer noise. As can be seen, the base case model prediction largely underestimates the experimental temperatures during the early stages of heating, thus confirming the earlier finding of Maloney et al. [1]. Fig. 3 shows a plateau region in the measured temperatures at the latter stages of heating during devolatilization and the base case assumption still largely underpredicts the measurements in this region. At the end of the 10 ms heating pulse, the measurements show a rapid cooling, whereas the base case assumption predicts a slow cooling. The temperature prediction using the measured shape and density information improved the fit somewhat during the entire particle residence time but failed to predict accurately the heating or cooling process.

Figures 4 and 5 present similar comparisons for all of the coal particles tested at two specific residence times (4 and 7 ms). These figures incorporate a broad range of heating intensities. The 4 ms (Fig. 4) heating time was chosen because at this time the particle surface temperature exceeded the pyrometer lower threshold limit (~ 800 K), but for most particles no significant volatile evolution was seen in the cinematographic records. The particles in the highest intensity group (particle # 34-39) in Table 1 showed some slight volatile evolution by 4 ms. The particles from the lowest intensity group (particle # 1-7) are not included in Figs. 4 and 5 because the temperature measurements for these particles at the 4 and 7 ms times were below the pyrometer measurement threshold. The solid lines in these figures represent the predicted temperatures for coal particles using the base case analysis described above. The triangles represent experimental temperature measurements and the solid squares represent corresponding model calculations using the measured particle shape information in the analysis. In each figure, the data has been segmented into three groups with each group being encircled to focus the readers attention and to illustrate some important points. In addition, since the middle grouping contained numerous points with significant scatter, four experiment-model point pairs were selected in these groups and connected by solid lines to highlight some patterns in the data.

Some important observations regarding the data in Figs. 4 and 5 include:

i. Model calculations using measured size and density information significantly underpredict the observed particle temperature. This observation is similar to that reported by Maloney and coworkers [1], who hypothesized that the differences between model and experiment could be due to poor understanding of coal thermodynamic and heat transfer properties and/or failure to account for particle shape considerations. The results presented in Figs. 4 and 5 indicate that even when particle shape is accounted for significant differences arise between measurement and model. We conclude that these differences are largely due to uncertainty in the coal thermodynamic and heat transfer properties in the model.

ii. Within each of the groupings, the measurements indicate a wide variation in observed temperatures even when the same nominal heat flux is applied. Within group two (the largest sample population tested) in both Figs. 4 and 5 the temperature spread for the groupings was in excess of 300 K at each of the measurement times chosen for comparison.

iii. A careful examination of each groupings in Figs. 4 and 5 shows a clear pattern in which the calculated particle temperatures mirror the experimental measured temperatures. This observation is perhaps most clearly illustrated in the last grouping on the right hand side of Fig. 5, but the pattern is consistent throughout each of the groupings. This observation indicates that, although the absolute temperature predictions are in error, much of the particle to particle variability observed within a given group can be explained by accounting for particle shape and density variations. For example, the calculated temperatures shown in the middle grouping in Fig. 5, predict a spread in temperatures of 275 K due to particle shape and density variations. The corresponding measurements indicate an observed temperature spread of 305 K. Making similar comparisons for each of the groupings, between 70 and 100 percent of the observed temperature spread in the Fig. 5 groupings can be accounted for in the model using the shape and density measurements made in this study. In Fig. 4, between 40 and 60 percent of the observed temperature spread can be accounted for using the measured shape and density values. An even larger percentage of the spread can be accounted for if the model thermal properties (primarily coal heat capacity) are adjusted to improve the fit between measurement and experiment.

CONCLUSIONS

Results presented for carbon spheres support the conclusion that the measurement and analysis methods applied here offer an excellent description of the energy balance for heating of single particles in the EDB. With well characterized materials of known properties, agreement between measurement and model of within 20 K is typical.

Large variations (several hundred degrees) are observed in coal particle temperature histories during rapid heating. These variations can be accounted for in large part due to particle to particle property (shape, mass, density) variations as demonstrated by the measurements and analysis presented above.

Even when accounting for particle to particle shape and density variations, model predictions in this study greatly underpredicted the observed temperature histories. Based on the results presented here and elsewhere [1] it is concluded that these discrepancies are largely due to uncertainty in the coal thermal properties (heat capacity and thermal conductivity) used to model coal combustion behavior. Future work in this laboratory will focus on using the measurement and analysis capabilities described here to evaluate these thermal properties under rapid heating conditions and this will be the subject of future publications.

ACKNOWLEDGEMENTS

This work was funded by Morgantown Energy Technology Center (METC), Department of Energy, under contract number DE - AP21- 92MC01595. Experiments were conducted at the Single Particle Laboratory, METC.

Per Nicci Gibson, contract no is for small purchase and ~~are~~ not loaded to PADS

NOMENCLATURE

A	particle cross-sectional area (μm^2)
C	particle heat capacity (cal g^{-1} K^{-1})
C_d/m	particle drag coefficient/mass ratio (sec^{-1})
d	particle diameter (μm)
h	heat transfer coefficient at particle surface (cal s^{-1} cm^{-1} K^{-1})
I	intensity of the laser (W cm^{-2})
K	thermal conductivity of particle (cal s^{-1} cm^{-1} K^{-1})
k	thermal diffusivity of the surrounding fluid (cm^2 s^{-1})
m	particle mass (μg)
R	particle radius (cm)
r	radial position (cm)
S	surface area (μm^2)
T	particle temperature (K)
t	Time (s)

<u>Greek Symbols</u>

α	particle absorptivity at 1.06 µm wavelength
ϵ	particle emissivity over the entire blackbody spectrum
σ	Stefan-Boltzman constant (cal s^{-1} cm^{-2} K^{-4})
ρ	particle density (g cm^{-3})

<u>Subscripts:</u>

0	at time = 0
p	of the particle
S	at particle surface
v	of volume equivalent

REFERENCES

1. Maloney, D. J., Monazam, E. R., Woodruff, S. W., and Lawson, L. W., Combust. Flame 84: 210-220 (1991).

2. Solomon, P. R., Serio, M. A., Carangelo, R. M., and Markham, J. R., Fuel 65:182 (1986).

3. Fletcher, T. H., Combust. Sci. Technol. 63: 89, (1989).

4. Sampath, R., Measurement and Prediction of Temperature Histories for Single Coal particles Prior to and During Devolatilization, PhD Thesis, Department of Chemical Engineering, West Virginia University, 1994.

5. Maloney, D. J., Lawson, L. O., Fasching, G. E., and Monazam, E. R., Aerosol Sci. Technol. 22: 60-72 (1995).

6. Monazam, E. R. and Maloney, D. J., Combust. Flame 99: 733-741 (1994).

7. Hurt, R. H. and Mitchell, R. E., Twenty-Fourth Symposium (International) on Combustion, The Combustion Institute, Pittsburgh, 1992, p. 1223.

8. Maloney, D. J., Lawson, L. O., Fasching, G. E., and Monazam, E. R., Rev. Sci. Instrum. 66: 3615-3622 (1995).

9. Brenner, H., Chem. Eng. Sci. 19:519 (1964).

10. Merrick, D. Fuel 62:540 (1983).

11. Badzioch, S., Gregory, D. R., and Field, M. A., Fuel 43: 267 (1964).

12. Spann, J. F., Maloney, D. J., Lawson, W. F., and Casleton, K. H., Applied Optics 32: 2152 (1993).

TABLE 1. Shape, Mass, Density and Heat Flux Information for Coal Particles

particle #	Surface area dia, d_{sa} (μm)	Vol dia, d_v (μm)	Laser area dia, d_L (μm)	Side view dia, d_s (μm)	C_d/m (1/s)	mass m (μg)	density ρ (g/cm³)	I(ta) (W/cm²)	$S_p/2A_L$ ratio
1	117	109	120	107	27.5	0.81	1.19	247	1.9
2	123	119	132	115	19.5	1.14	1.29	229	1.7
3	118	110	114	100	26.0	0.87	1.25	228	2.1
4	125	115	121	128	25.0	0.97	1.22	275	2.1
5	137	126	137	129	23.0	1.16	1.11	266	2.0
6	106	102	105	107	26.5	0.72	1.30	239	2.0
7[a]	121	114	110	133	25.0	0.95	1.22	298	2.4
8	118	110	109	109	25.0	0.89	1.28	584	2.3
9	110	104	99	115	28.0	0.72	1.22	583	2.5
10	115	109	104	115	28.0	0.76	1.12	553	2.4
11	106	95	103	95	36.0	0.59	1.31	584	2.1
12	88	81	85	92	47.0	0.36	1.29	577	2.1
13[b]	121	113	121	120	28.0	0.82	1.09	707	2.0
14[c]	111	102	106	103	33.0	0.65	1.18	692	2.2
15[d]	106	98	111	97	34.0	0.60	1.22	607	1.8
16	103	98	106	93	33.0	0.57	1.16	941	1.9
17	127	119	123	112	27.0	0.88	1.00	966	2.1
18	107	101	107	103	32.0	0.61	1.13	992	2.0
19	105	102	105	105	31.0	0.61	1.09	934	2.0
20	108	104	114	109	29.0	0.66	1.12	949	1.8
21	121	115	120	118	27.0	0.82	1.03	966	2.0
22	95	90	95	92	41.0	0.43	1.13	941	2.0
23	133	122	117	112	26.0	1.02	1.07	957	2.6
24	138	125	125	106	26.0	1.07	1.05	968	2.4
25	105	100	97	108	35.0	0.56	1.07	945	2.3
26	118	101	112	98	43.0	0.62	1.16	927	2.2
27	118	114	120	114	27.0	0.83	1.07	938	1.9
28	120	114	125	113	27.0	0.81	1.04	943	1.8
29	124	115	123	98	29.0	0.83	1.05	975	2.0
30[b]	109	102	111	105	35.0	0.60	1.08	1104	1.9
31[c]	123	107	125	131	32.3	0.77	1.20	1092	1.9
32[d]	130	124	132	108	23.0	1.03	1.03	1017	1.9
33[a]	124	116	115	109	26.0	0.89	1.09	940	2.3
34	109	104	97	111	28.0	0.69	1.17	1357	2.5
35	134	125	130	136	21.0	1.20	1.17	1314	2.1
36	124	116	120	102	25.0	0.93	1.14	1340	2.1
37	134	122	133	126	22.0	1.21	1.27	1344	2.0
38	111	107	108	110	28.0	0.70	1.09	1380	2.1
39[a]	129	121	116	126	22.0	1.10	1.19	1324	2.5
avg	117	110	114	111	28.9	0.81	1.15		2.1
std	11	10	12	11	5.8	0.21	0.09		0.2

[a] temperature data not available; [b,c,d] 2,3,5 ms pulse-width experiments.
particle # 1-7 are intensity group1, 8-15 are intensity group2, 16-22 are intensity group3A, 23-33 are intensity group3B and 34-39 are intensity group4.

FIGURE CAPTIONS

Figure 1. Schematic Diagram of Measurement System.

Figure 2. Experiment Reproducibility and Model Bound for a Carbon Sphere: Validation of Instrumentation and Heat Transfer Analysis. Pulse Intensity = 606 - 654 W/cm^2, Duration 10 ms.

———— Experiment (Total 7 Lines)

-------------- Model (Upper & Lower Bound)

Figure 3. Comparison of Model Prediction with Experiment..

Time Averaged Heating Pulse Intensity = 941W/cm^2, Duration 10 ms.

———— Experiment (particle # 16)

------------- Model (Measured Shape and Density).

— — —— Base Case

Figure 4. Comparison of Base Case Prediction @ 4 ms with ■ Prediction Using Measured Shape and Density and ▲ Measured Temperatures; ___ Model: Base Case.

Figure 5. Comparison of Base Case Prediction @ 7 ms with ■ Prediction Using Measured Shape and Density and ▲ Measured Temperatures; ___ Model: Base Case.

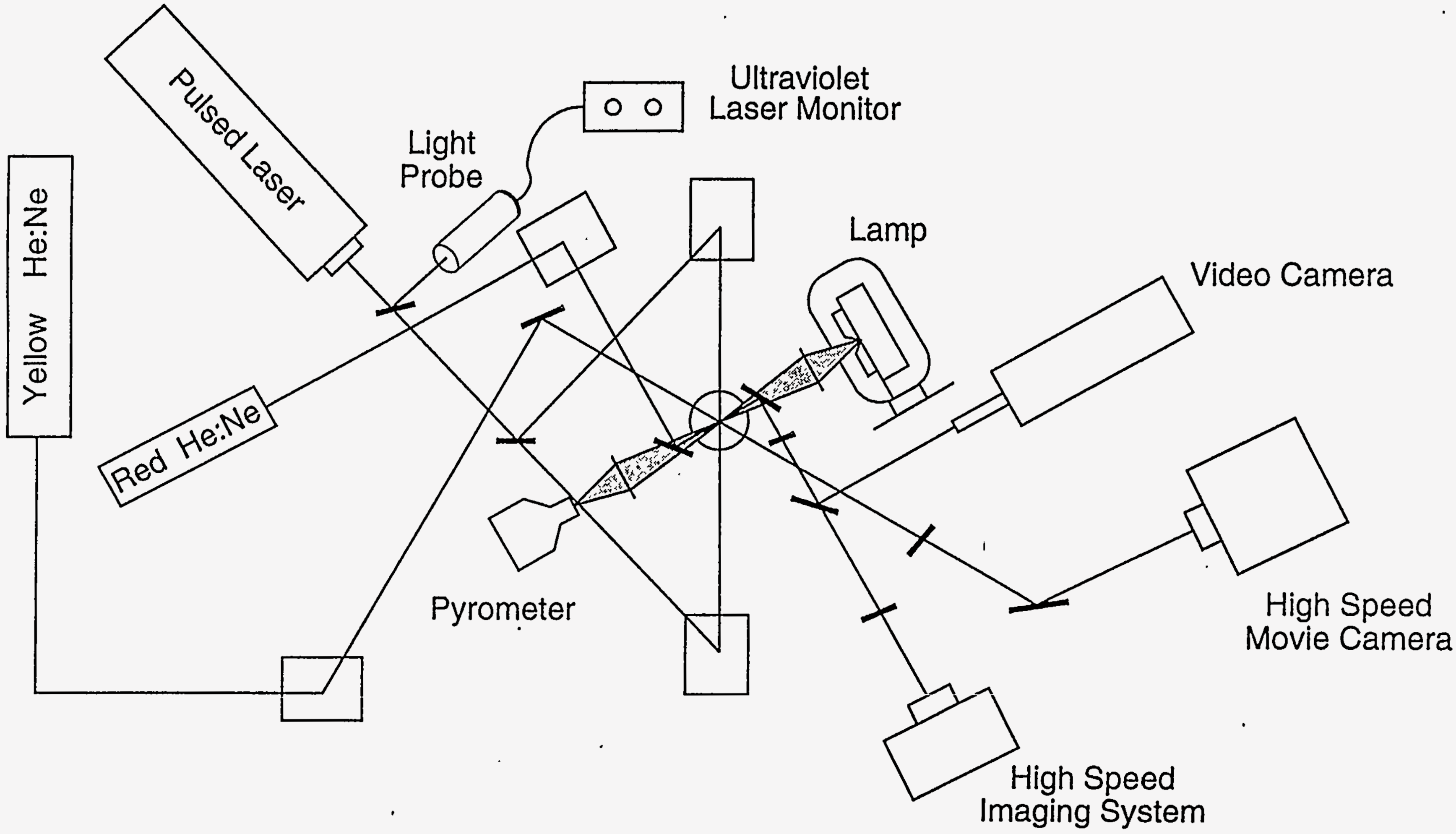
Pulsed Laser
Ultraviolet Laser Monitor
Light Probe
Yellow He:Ne
Lamp
Video Camera
Red He:Ne
Pyrometer
High Speed Movie Camera
High Speed Imaging System

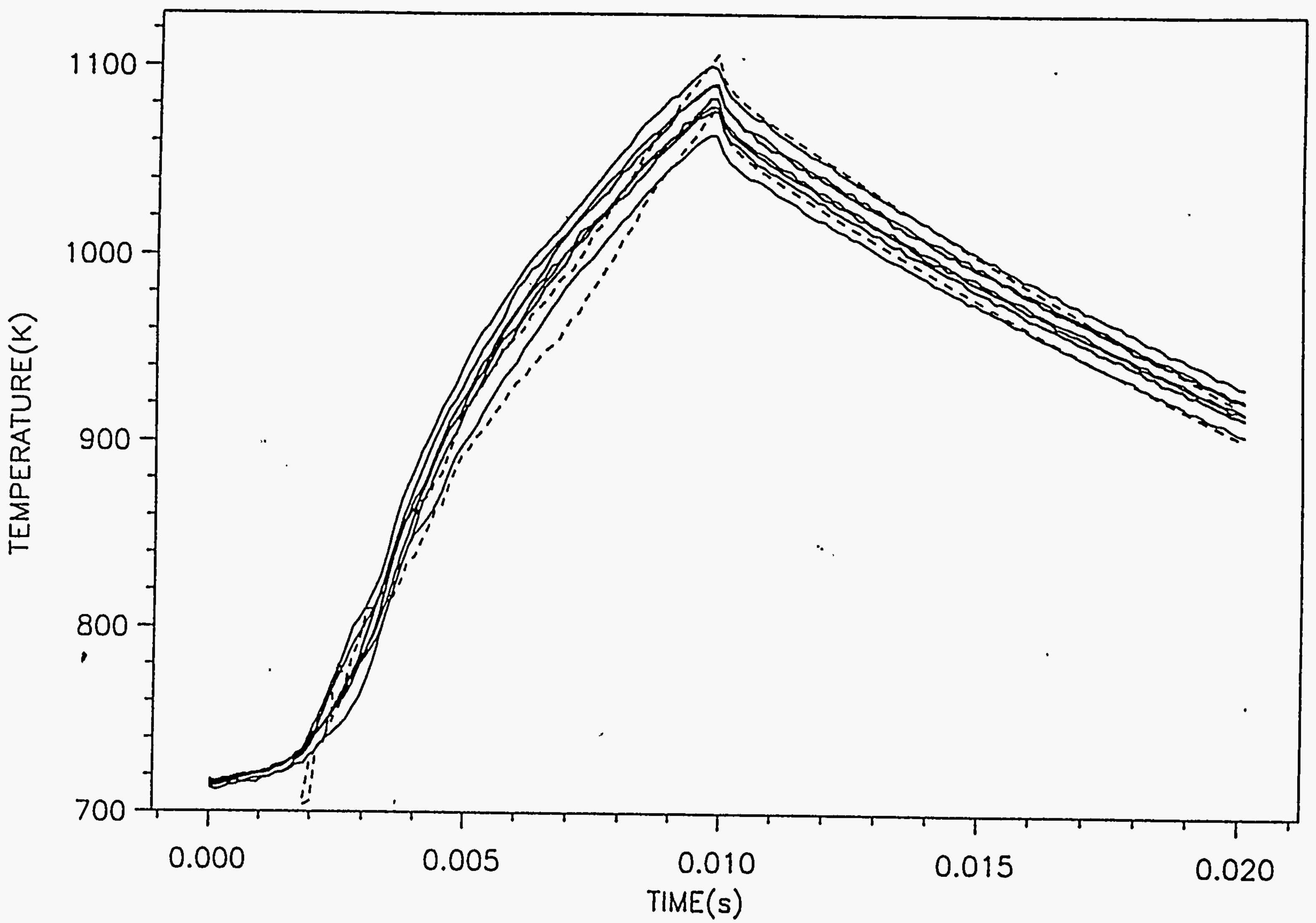
1100
1000
900
800
700
TEMPERATURE(K)
0.000
0.005
0.010
0.015
0.020
TIME(s)

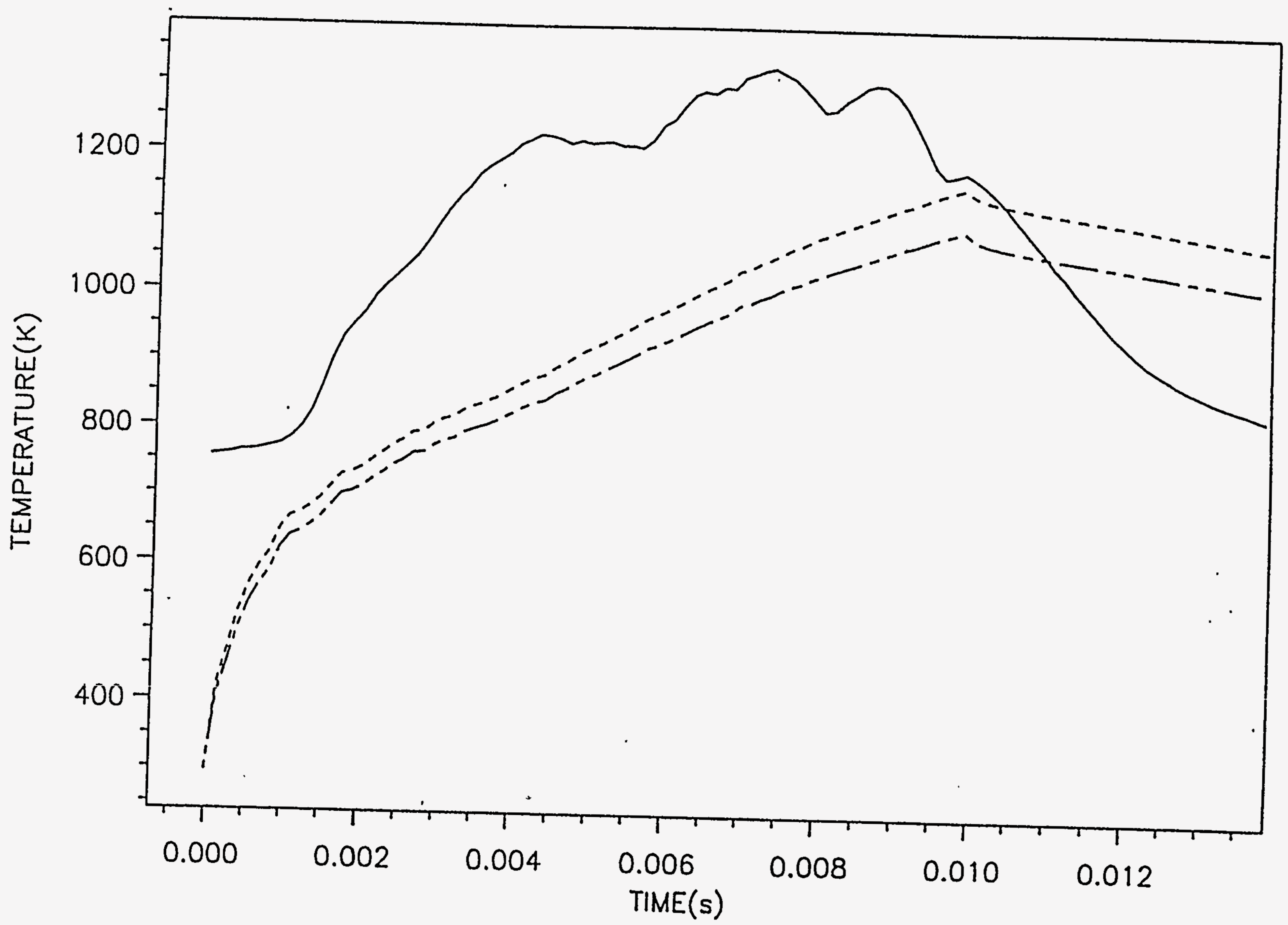

1200
1000
800
600
400
TEMPERATURE(K)
0.000
0.002
0.004
0.006
0.008
0.010
0.012
TIME(s)

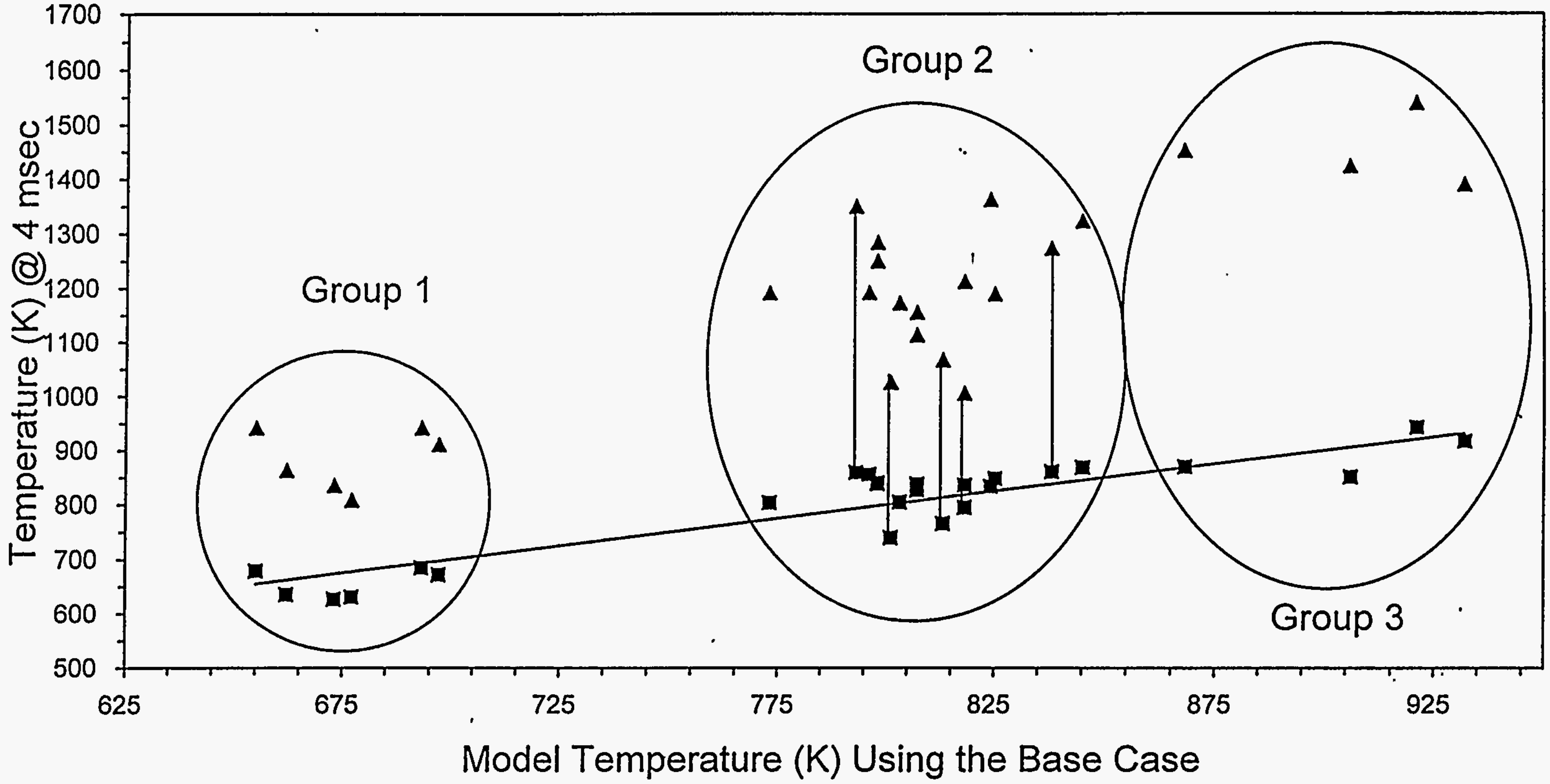

Group 1
Group 2
Group 3
Temperature (K) @ 4 msec
Model Temperature (K) Using the Base Case
1700
1600
1500
1400
1300
1200
1100
1000
900
800
700
600
500
625
675
725
775
825
875
925

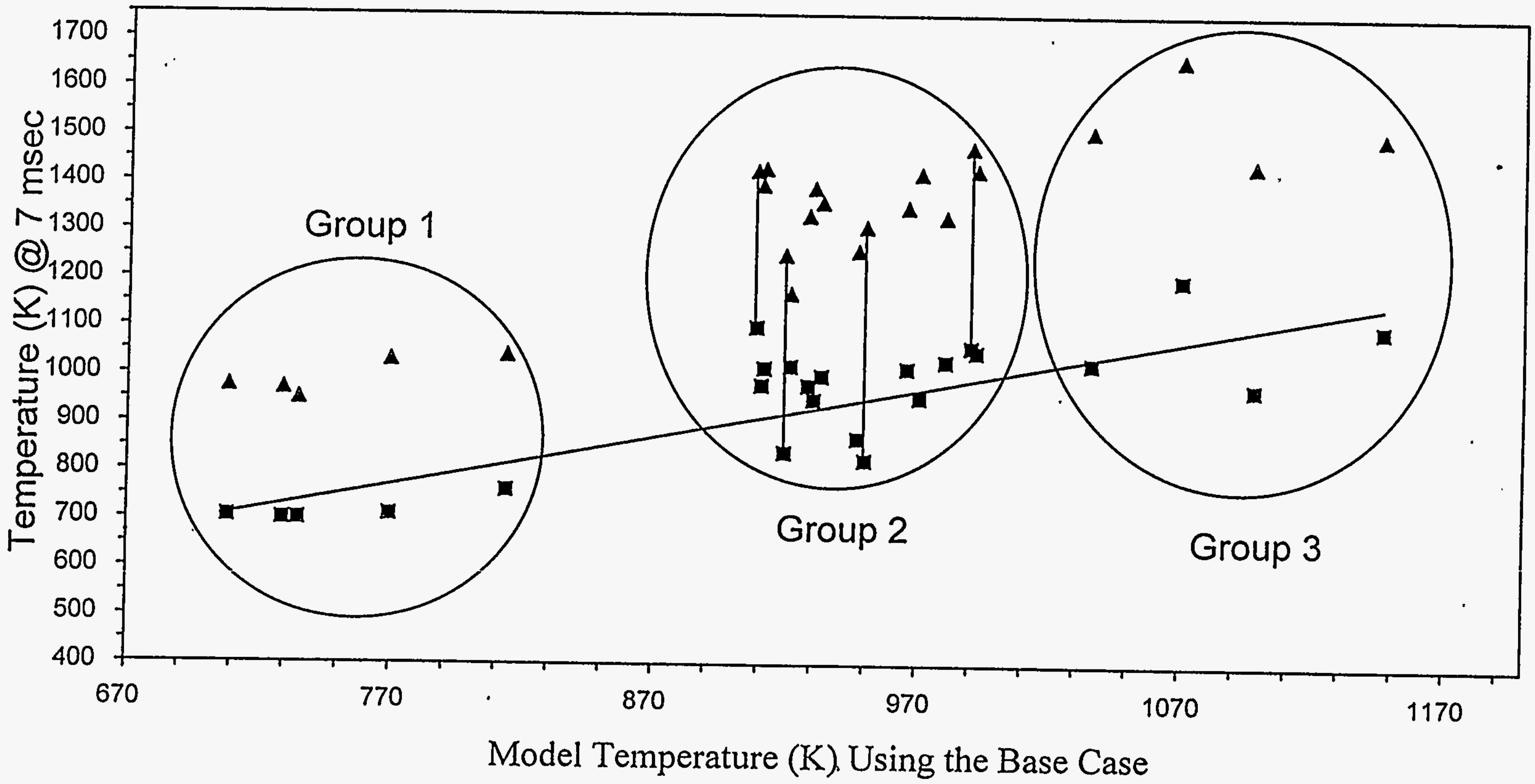
Temperature (K) @ 7 msec
1700
1600
1500
1400
1300
1200
1100
1000
900
800
700
600
500
400
670
770
870
970
1070
1170
Group 1
Group 2
Group 3
Model Temperature (K) Using the Base Case